

CHARACTERIZATION AND WEAR PERFORMANCE OF CrAgN THIN FILMS DEPOSITED ON Cr-V LEDEBURITIC TOOL STEEL

OCENA LASTNOSTI IN VEDENJE PRI OBRABI TANKIH PLASTI CrAgN, NANESENIH NA LEDEBURITNO ORODNO JEKLO Cr-V

Peter Jurči, Jana Bohovičová, Mária Hudáková, Pavel Bílek

Department of Materials, Faculty of Materials and Technology of the STU, Trnava, Paulínská 16, 917 24 Trnava, Slovak Republic
p.jurci@seznam.cz

Prejem rokopisa – received: 2013-02-14; sprejem za objavo – accepted for publication: 2013-05-28

Specimens made from Vanadis 6 cold-work tool steel were machined, ground, heat processed using a standard regime and finally mirror polished. After that they were layered with CrAgN. The Ag-content in the layers was chosen to be in mass fractions $w = 3\%$ and 15% . Microstructural analyses revealed that the CrN grew in a columnar manner. The addition of 3% Ag did not influence the manner of growth of the films, but the addition of 15% Ag made considerable changes to the film growth. Both the hardness and the Young's modulus were not influenced by the incorporation of 3% Ag, but the addition of 15% Ag reduced them. The layers with 3% Ag had excellent adhesion on the steel substrate. On the other hand, the addition of 15% Ag had a very negative impact on the coating adhesion. The films with the addition of 3% Ag had superior tribological properties against hard material (alumina) as well as against a soft counterpart (CuSn6 as-cast bronze), while those with 15% Ag were too soft and they underwent intensive wear.

Keywords: Vanadis 6 cold-work steel, PVD, chromium nitride, silver addition, tribological investigations

Vzorci, izdelani iz orodnega jekla Vanadis 6 za delo v hladnem, so bili obdelani, brušeni, toplotno obdelani po navadnem postopku in na koncu polirani do zrcalne površine. Nato je bil nanesen CrAgN. Količina v masnih deležih Ag v nanosu je bila izbrana 3% in 15% . Analize mikrostrukture so odkrile, da raste nanos v obliki stebriastih zrn. Dodatek 3% Ag ni vplival na način rasti nanosa, dodatek 15% Ag pa je povzročil občutne razlike v rasti nanosa. Oba, trdota in Youngov modul, nista bila odvisna od vnosa 3% Ag, dodatek 15% pa ju je zmanjšal. Nanosi s 3% Ag so imeli dobro oprijemljivost na podlagi iz jekla. Po drugi strani pa je dodatek 15% Ag močno poslabšal oprijemljivost nanosa. Nanosi s 3% Ag so imeli boljše tribološke lastnosti pri trdem materialu (aluminijev oksid), kot tudi pri mehkem (liti bron CuSn), medtem ko so bili tisti s 15% Ag premehkji in so izkazovali veliko obrabo.

Ključne besede: jeklo za delo v hladnem Vanadis 6, PVD, kromov nitrid, dodatek srebra, tribološke preiskave

1 INTRODUCTION

Thin CrN-based films have been developed over the past three decades. They quickly gained a great deal of interest and popularity in a variety of industrial applications due to their wear- and corrosion resistance and good cutting properties.¹⁻¹⁰

CrN films can be synthesized with a wide range of chemistries, phase constitutions and properties. A wide range of microhardness values of CrN-coatings, from 1500 HV for arc-vapour-deposited films^{8,11-13} up to 2450–2600 HV for those prepared by magnetron sputtering techniques¹⁴⁻¹⁷ can be obtained. In selected cases, for ultra-fine-grained films in particular, the microhardness of CrN-films can reach very high values, exceeding 3000 HV, as reported by Mayrhofer et al.¹⁸ It should be noted that the phase constitution of the films also plays a role in their microhardness – the majority of authors established a slightly higher hardness for the Cr₂N than for the CrN,¹⁹⁻²³ while it was only Nouveau et al.⁹ and Beger et al.²⁴ who reported the opposite tendency. The films prepared by high-power pulsed-magnetron sputtering (HIPIMS) also have a high hardness.²⁵ The Young's modulus E of CrN-based films can also be varied over a

wide range, from 188 GPa to 400 GPa, depending on the negative substrate bias, the substrate temperature and the substrate nature (chemistry, phase constitution, hardness).^{14,16,17,26} The formation of high internal stresses, mostly compressive, is one of the key problems connected with film growth on substrates. The stress intensity depends mainly on the substrate bias voltage – the application of low bias voltage produces internal stresses of around 2 GPa,^{19,25} while the stresses can reach over 4 GPa when a negative substrate bias higher than 75 V is used for the deposition.^{17,27} In any case, too high internal stresses influence the adhesion of the films negatively. The reduction of the stresses is possible through the post-deposition annealing of the films, which led to improved adhesion.^{13,28} The difference in the mechanical (hardness) and physical (Young's modulus, thermal expansion coefficient, etc.) properties can cause serious problems with respect to the adhesion of the coatings to the substrate. Generally, a good adhesion can be achieved when ledeburitic steels or cemented carbides are used as a substrate,^{10,13,27,29,30} due to their high hardness. The adhesion also increases as the portion of the phase CrN decreases and Cr₂N and/or (Cr) solid solution increases.^{12,17,28}

The tribological properties of CrN-based films, however, cannot be changed over a sufficiently wide range. External lubrication is one of the possible ways how to improve the tribological behaviour of the films, but commercially available lubricants (oxides, molybdenum disulfide, graphite) exhibit considerable shortcomings. Graphite and molybdenum disulfide, for instance, undergo oxidation above 300 °C and, hence they degrade rapidly. Furthermore, metallic oxides, on the other hand, cannot be used at low temperatures since they exhibit an abrasive behaviour.

This is why self-lubricating composite films have been a subject of scientific interest in the past few years. These films combine a hard wear-resistant matrix (mostly formed by nitrides or carbo-nitrides) with soft lubricious phases that provide lubricious layer at room and elevated temperatures.

Silver is the most common addition used with transition-metal (TM) nitride thin films. It possesses a stable chemical behaviour and can exhibit self-lubricating properties due to its low shear strength. In addition it is known that silver is capable of migrating to the free surface, providing lubrication above 300 °C. Several investigations were focused on the TM-based ceramic films with the addition of silver, deposited on various substrates. The findings on the effect of Ag addition can be summarized as follows. The addition of silver can lead to an alteration in the growth of CrN-based films, as reported for instance by Mulligan et al.³¹ There is a relatively good consensus on the lowering of the friction coefficient at operating temperatures in the range 300–500 °C.^{31–37} The nature of this phenomenon is also well known. Silver is almost completely insoluble in CrN and forms nanoparticles in the basic CrN-compound. The Ag atoms can easily migrate to the free surface at elevated temperatures, form lubricious grains there, and thereby reduce the friction force significantly. On the other hand, the tribological properties of Ag-containing films differ significantly above 500 °C, whereas the nature of the TM nitride matrix is a key factor influencing their improvement³⁴ or deterioration.^{32,33,35} The choice of an "optimal" silver addition, from point of view of tribological performance, into the basic film is not in doubt – many authors evaluated films with very high silver contents, e.g., above the mole fraction 20 %^{31–33,35–37} although it seems that a much lower silver addition can lead to superior tribological parameters.^{38,39} One can assume that silver, as a naturally soft metal, should reduce both the hardness and the Young's modulus of the films. However, some experimental works established either "no effect" of silver or a slight increase of the hardness.^{38,39} The information on the effect of silver on the adhesion of films is lacking – one of the possible reasons is that various materials with completely different properties were used as substrates. Kostenbauer et al.⁴⁰ made very important observations. They investigated the stress development in multilayered

TiN/Ag films with a different modulation period. The principal finding was that the stresses in all the multilayers decreased up to a temperature of 380 °C, followed by a plateau above this temperature. The authors attributed this behaviour to the fact that further stresses were relieved by the plastic deformation of silver interlayers. Based on these investigations, one can also assume that soft silver particles can also effectively relieve the internal residual stresses in the CrN-films, which can make a substantial contribution to the better adhesion of CrN-films and their improved wear behaviour.

Various materials (silicon wafers, carbon steels, nickel superalloys and stainless steels) have been used as substrates for CrAgN films, but not including ledeburitic steels. These materials, however, belong to the most important tool steels, which are used in many industrial operations, due to their good combination of structure and mechanical properties. Moreover, they can be changed using variations of heat-treatment parameters across a wide range.^{41–43} The main challenge to perform the experimental works was thus to minimize the gap in knowledge, e.g., to evaluate what happens when P/M ledeburitic steels are coated with CrAgN. The current paper attempts to put together the experimental results on the development of adaptive nanocomposite CrAgN coatings on the Vanadis 6 Cr-V ledeburitic tool steel and to make a comprehensive report on the basic coating characteristics, like microstructure, hardness, Young's modulus, wear resistance, friction coefficient, as a function of the silver content and deposition temperature, with a small look into the near future at the end of the paper.

2 EXPERIMENTAL

2.1 Material and processing

The experimental material was the powder metallurgical ledeburitic steel Vanadis 6 with nominally mass fractions: $w(\text{C}) = 2.1 \%$, $w(\text{Si}) = 1.0 \%$, $w(\text{Mn}) = 0.4 \%$, $w(\text{Cr}) = 6.8 \%$, $w(\text{Mo}) = 1.5 \%$, $w(\text{V}) = 5.4 \%$ and Fe as balance. Two types of samples were made from the experimental material. The first ones were plates of 40 mm × 20 mm × 5 mm intended for the wear testing. The second samples were un-notched Charpy impact-test specimens (55 mm × 10 mm × 10 mm). After rough machining to the semi-final dimensions, the samples were subjected to a standard heat-treatment procedure consisting of the following steps: vacuum austenitizing up to the final temperature of 1050 °C, followed by nitrogen gas quenching (5 bar) and twice tempering. Each tempering cycle was conducted at 530 °C for 2 h. The resulting as-tempered hardness of the material was 724 HV (10). After the heat treatment, all the samples were fine ground and polished with a diamond suspension to a mirror finish.

The CrN- and CrAgN coatings were deposited in a magnetron sputter deposition system, in a pulse regime

with a frequency of 40 kHz. It should be noted that no adhesion inter-layer (like pure CrN) was deposited prior to the formation of either the CrN or CrAgN films, in order to highlight the differences in the adhesion of the films themselves. Two targets, positioned opposite to each other, were used. For the deposition of CrN, two targets from pure chromium (99.9 % Cr) were used. The target output power was adjusted to 2.9 kW for each cathode. For the deposition of the silver-containing films, one silver cathode (99.98 %) was inserted into the processing chamber instead of one chromium target. In these trials, the cathode output power was 5.8 kW on the chromium cathode. On the silver cathode, the output powers were 0.1 kW and 0.45 kW in order to produce the silver contents in the coating of 3 % and 15 % (mole fractions 1.3 % and 6 %), respectively. Two deposition temperatures were used. The first one was 250 °C. To achieve that, the samples were heated using resistive heaters during the sputter-cleaning step. Afterwards, the substrate temperature of 250 °C was kept constant by ion bombardment only. The second deposition temperature was 500 °C. It was achieved using resistive heaters placed on the internal walls of the processing chamber. The processes were carried out in a low-pressure atmosphere (0.15 mbar), containing pure nitrogen and argon (both of 99.999 % of purity), in a ratio of 1 : 4.5.

The specimens were ultrasonically degreased in acetone and loaded into the processing chamber. They were placed between the targets on rotating holders, with a rotation speed of 3 r/min. Just prior to the deposition, the substrates were sputter cleaned in an argon low-pressure atmosphere for 15 min. The substrate temperature was 250 °C for the cleaning. A negative substrate bias of 200 V was used for the sputter cleaning and that of 100 V for the deposition. The total deposition time was 6 h.

2.2 Investigation methods

The microstructure of the substrate material was documented using a light microscope ZEISS NEOPHOT 32 and a field-emission scanning electron microscope (SEM) JEOL JSM-7600F operated at an accelerating voltage of 15 kV. Metallographic samples were prepared using a standard preparation technique (rough and fine grinding, polishing by diamond suspension) and finally etched with Vilella-Bain reagent.

The microstructure of the counterface materials was recorded using a light microscope ZEISS NEOPHOT 32 after a standard metallographic preparation.

Microstructural analyses of coatings were completed on the fracture surfaces of coated Charpy impact specimens. The material was immersed into liquid nitrogen for 20 min. and then broken down. The fracture surfaces were cleaned ultrasonically with acetone before observation, in order to remove any possible contamination of the material. A scanning electron microscope JEOL JSM-7600F operating with the same parameters was used for the analyses.

The nanohardness and the Young's modulus (E) of the coatings were determined using a nano-indenter under a normal load of 20 mN, for a NanoTest (Micro Materials Ltd) nanohardness tester equipped with a Berkovich indenter. Ten indentations were made for each coating applied and the mean value and the standard deviation were calculated from the measured values. The penetration depth (loading) of the indenter was chosen so as to not exceed one tenth of the total coating thickness, in order to avoid the influence of the substrate on the measured nanohardness.

The adhesion of the coatings on the substrate was evaluated using a CSM Revetest scratch-tester. The scratches were made under progressively increasing loads from 1 N to 100 N, with a loading rate of 50 N/min. A standard Rockwell diamond indenter with a tip radius of 200 μm was used. Five measurements were made on each specimen and the mean value of the adhesion, represented by the L_{c1} and L_{c2} critical loads, respectively, was calculated. The critical loads were determined by the recording of an acoustic emission signal as well as by viewing the scratches on the light micrographs. The L_{c1} critical load corresponded to the occurrence of the first inhomogeneities in the coating and the L_{c2} critical load was determined as the load when 50 % of the coating was removed from the substrate, unless otherwise discussed in the text.

The tribological properties of the coatings were measured using the CSM Pin-on-disc tribometer at ambient and elevated temperatures up to 500 °C. Balls of 6 mm in diameter, made from sintered alumina and CuSn6 bronze (as-cast structure, hardness of 149 HV (10)) were used for testing at all the temperatures. The balls made from heat-processed 100Cr6 ball-bearing steel (hardness of 700 HV (10)) were used, but for the testing at ambient temperature only. The experiments were conducted in laboratory air, at a relative humidity of 40–50 %. No external lubricant was added during the measurements. The normal loading used for the investigations was 1 N. For each measurement, the number of cycles was 5100, e.g., the total sliding distance was 100 m at the sliding radius of 5 mm. After the testing, the wear-track widths were measured on a light microscope ZEISS NEOPHOT 32 at a magnification of 50-times. Ten measurements were made on each track and the mean value, which was used for further evaluation, was calculated. The volume loss of the coated samples was calculated from the width of the wear tracks using the formula:⁴⁴

$$V_1 = 2\pi R \left[\frac{r^2}{\sin\left(\frac{d}{2r}\right)} \right] - \frac{d}{4} \sqrt{4r^2 - d^2}$$

where R is the wear-scar radius, d is the mean value of the wear-track width, and r is the radius of the ball counterface.

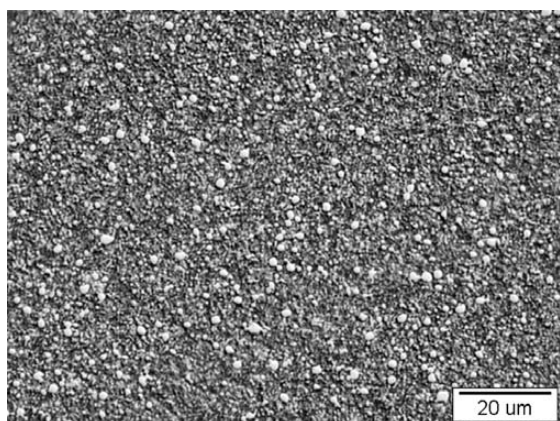


Figure 1: Light micrograph showing the microstructure of the PM ledeburitic steel Vanadis 6 substrate in the as-quenched and tempered state

Slika 1: Posnetek mikrostrukture kaljene in popuščene podlage iz PM ledeburitnega jekla Vanadis 6

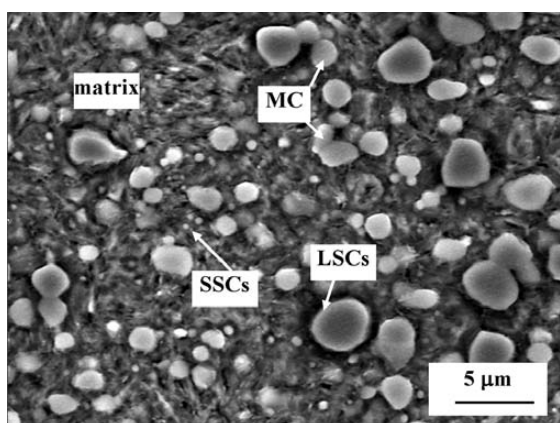


Figure 2: SEM micrograph showing detailed microstructure of PM ledeburitic steel Vanadis 6 substrate in the as-quenched and tempered state

Slika 2: SEM-posnetek detajla mikrostrukture kaljene in popuščene podlage iz PM ledeburitnega jekla Vanadis 6

The wear rate was then derived from the volume-loss calculation, using the formula:⁴⁴

$$W = \frac{V_1}{l \times F_n}$$

where W is the wear rate, l is the sliding distance (m), F_n is the applied normal load and V_1 is the volume loss.

3 RESULTS AND DISCUSSION

3.1 Substrate characterization

The microstructure of the substrate material after the heat treatment is shown in **Figures 1** and **2**, respectively. The light micrograph (**Figure 1**) shows that the material consists of a matrix, formed with tempered martensite and fine carbides, uniformly distributed throughout the matrix. The carbides are of two types (**Figure 2**). The MC-phase (medium-sized particles) mostly forms the eutectic part of the carbides. The second carbide type is the M_7C_3 . The M_7C_3 -phase underwent dissolution in the austenite during the heat processing, being responsible for the saturation of the austenite with the carbon and alloying elements.⁴⁵ The other part of the M_7C_3 -carbides (designated as large secondary carbides (LSCs) and small secondary carbides (SSCs), and an almost complete amount of MC phase remained undissolved. After the heat treatment, the average hardness of the material was 724 HV (10).

3.2 Microstructure of the films

Figure 3 shows cross-sectional secondary-electron micrographs from all the developed films. The thickness of the CrN film without any silver addition was 4.3 μm (**Figure 3a**). This corresponds to a growth rate of 720 nm/h. The addition of 3 % of Ag did not change the

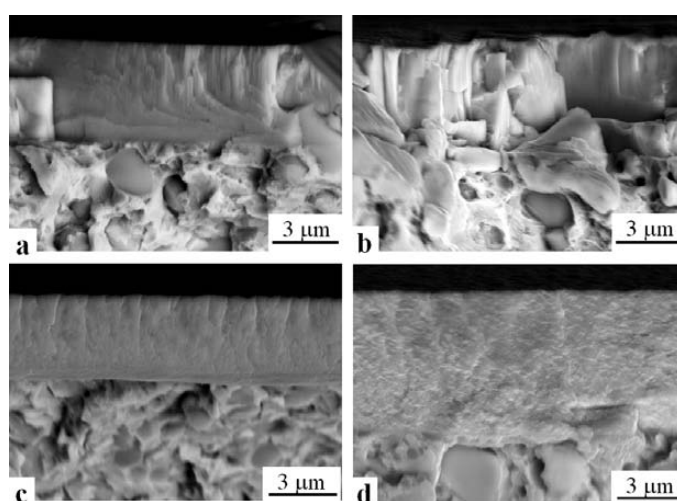


Figure 3: SEM micrographs showing the microstructure of developed films: a) CrN, deposition at 250 °C, b) CrAg3N, deposition temperature of 250 °C, c) CrAg3N, deposition temperature of 500 °C and d) CrAg15N, deposition temperature of 500 °C^{47,48}

Slika 3: SEM-posnetki mikrostrukture razvoja plasti: a) nanos CrN pri 250 °C, b) CrAg3N, temperatura nanašanja 250 °C, c) CrAg3N, temperatura nanašanja 500 °C in d) CrAg15N, temperatura nanašanja 500 °C^{47,48}

thickness (and the growth rate) of the films (**Figures 3b** and **3c**). On the other hand, the addition of 15 % Ag accelerated the growth rate of the film to 1050 nm/h and, as a result, this film had a thickness of 6.3 μm (**Figure 3d**). It should be noted that these results are inconsistent with other literature data. Yao et al.,⁴⁶ for instance, reported a decreased film thickness with a Ag addition. However, they have used completely different experimental setup for the coating deposition, which makes the results only roughly comparable. Our results, on the other hand, indicate that small addition of silver does not influence the growth rate of the films, which was confirmed recently.^{47,48}

The pure CrN-based film, formed at 250 °C, grew in a columnar manner with clearly visible individual crystallites (**Figure 3a**). This type of layer growth is typical for magnetron sputtered CrN-films formed over a wide range of deposition parameters, as reported previously.⁴⁹ The addition of 3 % Ag into the CrN, formed at the same temperature, did not change the growth mechanism of the layer significantly (**Figure 3b**). The temperature effect on the layer growth for the films with 3 % Ag addition is visible on the micrograph in **Figure 3c**. It is clearly visible that the higher deposition temperature does not influence the growth manner. **Figure 3d** shows the microstructure of the film with 15 % Ag addition. The secondary-electron-mode detection yields clearly visible

contrast between high atomic Ag (bright) and the surrounding CrN base. It is also clear that no individual crystals of CrN were formed. Therefore, it is clear that a small Ag addition does not change the growth manner of the film, while a higher Ag content incorporated into the CrN matrix has a considerable impact on that.

Figure 4 brings representative SEM micrographs of the deposited films and corresponding EDS maps of silver. These pictures indicate that the surface microstructure is strongly influenced by introducing silver into the basic CrN-film. The surface of pure CrN (**Figure 4a**) exhibits a clearly visible, non-uniform structure, made up of two types of features. The first type of feature is the semi-equiaxed grains (SEG) with a size of 0.4–0.7 μm. This feature makes up around 90 % the surface and can be referred to as a "matrix". In this "matrix", several formations that can be described as a cauliflower-like (CFL) structure are embedded. Similar surface structure of chromium nitride films has already been reported and discussed by Zhao et al.⁵⁰ They established that the combination of "equiaxially grained" (or faceted) and CFL structures is typical for two-phase (CrN and Cr₂N) films.

The addition of 3 % Ag into the chromium nitride basic film causes a significant refinement in the grain size of the individual crystals (**Figure 4b**). No individual silver grains but inhomogeneities in the chemical composition throughout the micrograph became visible (**Figure 4c**).

The SEM micrograph in **Figure 4d** and the corresponding EDS mapping of Ag (**Figure 4e**), show that silver forms agglomerates (appearing in bright contrast due to their higher secondary-electron yield versus CrN) on the surface at a concentration of 15 %. The size of the silver agglomerates is well below 1 μm.

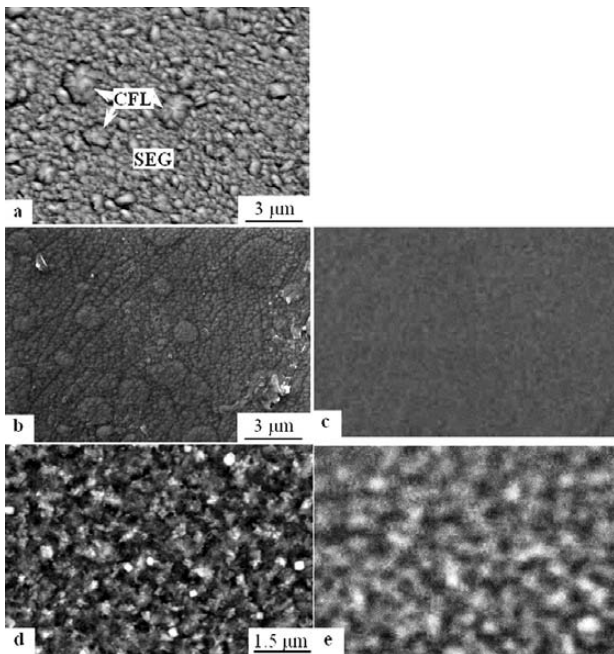


Figure 4: Plan-view SEM micrographs showing the surface microstructure of deposited films: a) CrN, deposition at 250 °C, b) CrAg₃N, deposition temperature of 250 °C, c) corresponding EDS-map of silver, d) CrAg₁₅N, deposition temperature of 500 °C and e) corresponding EDS-map of silver

Slika 4: SEM-posnetki površine, ki prikazuje mikrostrukturo nanosene plasti: a) CrN, nanešen pri 250 °C, b) CrAg₃N, temperatura nanašanja 250 °C, c) EDS-razporeditev srebra, d) CrAg₁₅N, temperatura nanašanja 500 °C in e) EDS-razporeditev srebra

3.3 Mechanical properties of the films

The microhardness of pure CrN was (16.79 ± 1.49) GPa (**Table 1**). The microhardness of films containing 3 % Ag was only very slightly lower than that of the film that does not contain silver. Furthermore, the microhardness of these films was almost the same, e.g., the deposition temperature plays only a very minor role with respect to the coating hardness. The addition of 15 % Ag, on the contrary, led to a substantial hardness reduction, i.e., (11.43 ± 0.61) GPa. This may be explained by

Table 1: Mechanical properties of investigated films. The circled values (●) were obtained in a previous study⁴⁷

Tabela 1: Mehanske lastnosti preiskovanih nanosov. Vrednosti, označene z (●), so iz vira⁴⁷

Coating/deposition temperature	Hardness (GPa)	Young's modulus E/GPa
CrN/250 °C ●	16.79 ± 1.49	244 ± 15
CrAg ₃ N/250 °C ●	15.97 ± 1.44	241 ± 9
CrAg ₃ N/500 °C	16.13 ± 1.83	246 ± 17
CrAg ₁₅ N/500 °C	11.43 ± 0.61	204 ± 6

the fact that silver is a very soft metal and its agglomerates embedded in the CrN matrix cause softening of the film. These observations are very consistent with other experimental works. Yao et al.⁴⁶ reported only a very slight Knoop hardness decrease for magnetron sputtered nanocomposite coatings with very small silver additions. Mulligan et al.³¹ established a much more remarkable hardness decrease, but they added the mole fraction of Ag 22 % (e.g., a much larger amount than that used in this study).

The Young's modulus, E , of the CrN and CrAg3N films was of about 240 GPa (Table 1). The E value ranges, in addition, overlap considerably. The addition of 15 % of silver to the basic film, on the other hand, tends towards a decrease of the Young's modulus. The information on the impact of the silver addition on the Young's modulus is lacking in the literature. Only Aouadi and his co-workers³⁸ reported a decreased

Young's modulus with an increased amount of silver in magnetron-sputtered YSZ-based films. The fact that the Young's modulus reduces with the addition of silver can be considered as natural, since silver had a much lower E (around 79 GPa) than chromium nitride (over 200 GPa in most cases^{14,16,17}). However, at very small silver additions, there is almost no impact of silver on the Young's modulus, as indicated in Table 1. It seems that there is a threshold below which no impact of the silver on the Young's modulus can be expected and, above which the addition of silver leads to a substantial lowering of the E .

One can believe that the effect of the size and the distribution of silver particles can also play a role in the mechanical behaviour of the coatings. However, there is no relevant information on the impact of these structural parameters on the mechanical properties of the films yet. These investigations can be considered as a challenging factor for further investigations.

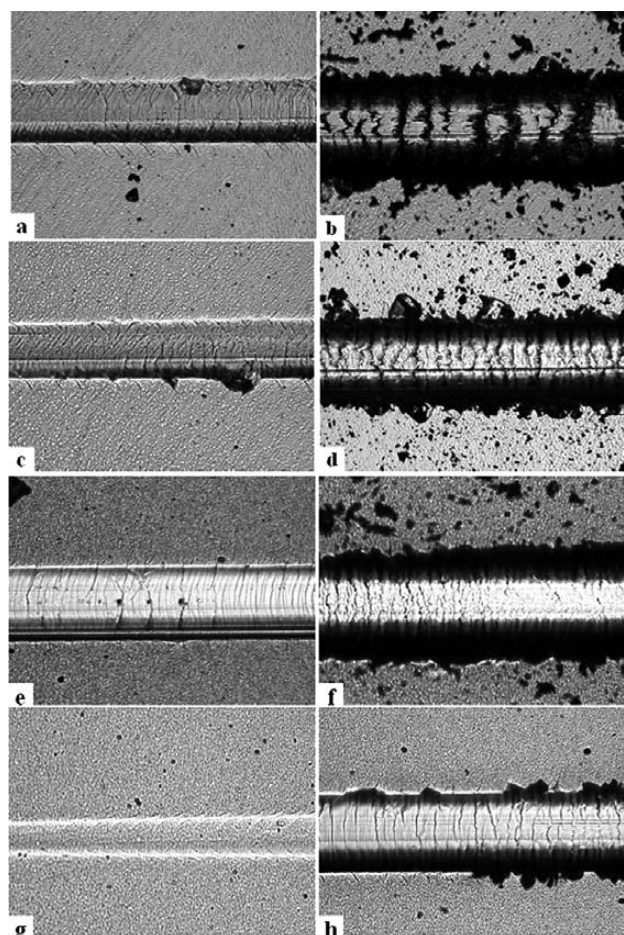


Figure 5: Light micrographs showing the failures after scratch testing: a) CrN, deposition temperature of 250 °C, L_{c1} , b) L_{c2} , c) CrAg3N, deposition temperature of 250 °C, L_{c1} , d) L_{c2} , e) CrAg3N, deposition temperature of 500 °C, L_{c1} , f) L_{c2} , g) CrAg15N, deposition temperature of 500 °C, L_{c1} , h) L_{c2} ^{47,48}

Slika 5: Svetlobni posnetki napak, nastalih pri preizkusu razenja: a) CrN, temperatura nanašanja 250 °C, L_{c1} , b) L_{c2} , c) CrAg3N, temperatura nanašanja 250 °C, L_{c1} , d) L_{c2} , e) CrAg3N, temperatura nanašanja 500 °C, L_{c1} , f) L_{c2} , g) CrAg15N, temperatura nanašanja 500 °C, L_{c1} , h) L_{c2} ^{47,48}

3.4 Adhesion of the films

After the scratch-test, the failure of the pure chromium nitride film begins with semi-circular tensile cracking (Figure 5a). The first cracks were observed at a normal load of around 24 N (L_{c1}). The "total" failure of the chromium nitride film is shown in Figure 5b. It is manifested by many parallel cracks visible in the scratch, where about 50 % of the coating is removed from the substrate. The typical load range when this phenomenon occurred was 40–45 N.

The slightly softer CrAg3N film deposited at 250 °C also failed due to the presence of semi-circular tensile cracks. However, the distance between the first cracks is larger than that in the pure chromium nitride and some of the cracks stopped their propagation through the scratch (Figure 5c). The critical load at which these phenomena first occurred was around 23 N (Table 2). Figure 5d shows the total failure of the CrAgN film grown at 250 °C. It is evident that some of the parallel cracks stopped their propagation through the film, which suggests that the coating can store a larger amount of plastic deformation energy preceding the failure. This assumption is supported by the fact that the "total" failure of the film was detected at a load higher than that of pure chromium nitride (Table 2).⁴⁷

Table 2: Critical loads for a defined degree of coatings failure⁴⁷

Tabela 2: Kritične obremenitve za opredeljeno stopnjo poškodbe nanosa⁴⁷

Coating/deposition temperature	L_{c1}/N	L_{c2}/N
CrN/250 °C	24.5 ± 1.7	42.7 ± 4.4
CrAg3N/250 °C	23.4 ± 5.9	52.2 ± 5.9
CrAg3N/500 °C	46.9 ± 8.1	82.6 ± 8.4
CrAg15N/500 °C	6.4 ± 0.6	44.1 ± 6.3

For the film with 3 % Ag addition, grown at a substrate temperature of 500 °C, the first indication of

coating damage occurred at an average loading of around 47 N (L_{c1}). Coating damage begins with the appearance of semi-circular tensile cracks, e.g., it looks to be similar to that of the coating deposited at a lower temperature (Figure 5e). The "total" failure of the film is in Figure 5f. It is typical, with the occurrence of many parallel micro-cracks inside the scratch track. Some of them stopped their propagation during the testing. Also, it is shown that part of the track (the left-hand side of the micrograph) does not exhibit visible cracks. Here, no typical "coating damage" was observed (50 % of the coating removed). The typical load when this symptom occurred ranged between 74 N and 88 N (L_{c2}).

The beginning of the failure of the film containing 15 % Ag cannot easily be found. Figure 5g shows a scratch track at a relatively low loading range (around 6.4 N), where the critical load L_{c1} was determined. However, neither tensile cracking nor spallation of the film has been observed at low loading. What was determined was only that the film underwent a local plastic deformation with clearly visible, semi-circular deformation zones (arrow designated). These zones are widely spaced, which suggests that the film is capable of storing a relatively large amount of plastic energy before failing cohesively. Typical symptoms for the "total" failure of the coating have not been detected, in a similar way to the film with 3 % Ag (Figure 5f). The scratch track contained many parallel cracks and microcracks when subjected to higher loads (Figure 5h). Moreover, the first symptoms of chipping were detected as being adjacent to the scratch track at a normal load of 44.1 N.

The fact that a high silver content tends to worsen adhesion of the film is consistent with Yao's findings,⁴⁶ where a very slight adhesion decrease with increasing silver content has been reported. However, the experimental setup used was different in this work, i.e., an M2-type high-speed steel with unknown hardness and heat treatment state was used as a substrate instead of Vanadis 6, another deposition system was applied for the coating growth and, finally, no details of the scratch testing were reported. All these facts make the results almost incomparable. What can be suggested is that the high silver content makes the coating too soft and very sensitive to the failure at higher loading.

Moreover, the addition of 3 % silver increased the adhesion of the films in our work, particularly when a temperature of 500 °C was used for the deposition. Here, Kostenbauer's findings,⁴⁰ that the intrinsic stresses in silver-containing multilayer coatings are relieved above 380 °C, can give a correct explanation. It is known that the deposition of chromium nitride films, which do not contain silver, leads to the formation of high intrinsic stresses, exceeding 4 GPa.^{17,19,25,27} They can be lowered by several methods. One of them is a so-called "post-deposition annealing", which can result in the increased adhesion performance of the films.¹³ The second suitable method is the incorporation of a soft and insoluble phase

(pure silver for instance) into the chromium nitride. It can be assumed that such a phase would be capable of relaxing the stresses during the deposition of the films. Based on this assumption, a distinctively higher adhesion strength of the films that contain 3 % Ag seems to be logical.

3.5 Tribological investigations

Figure 6 gives an overview of the friction coefficients μ resulting from testing at room temperature for all the used counterparts. The pure CrN film has a $\mu = 0.378$ when tested against alumina. The CrAg3N films formed at 250 °C and 500 °C had average friction coefficients of 0.389 and 0.373, respectively. The lowest average μ was recorded for the film containing 15 % Ag, i.e., 0.365. Therefore, one can conclude that almost no positive effect of the silver addition can be found when an alumina ball is used.

Generally, the testing against 100 Cr6 ball-bearing steel gave a slightly higher μ compared to the alumina. The pure CrN film had average of $\mu = 0.425$. The silver-containing-films had a slightly lowered friction coefficient, e.g., around 0.4, but it should be noted that the friction-coefficient value ranges overlap. Thus, one would conclude that no positive impact of the silver on the friction coefficient of CrN against 100 Cr6 steel has been found, in a similar way to the case of alumina ball counterpart.

Testing against a CuSn6 bronze ball gave a lower friction coefficient. The pure CrN film had a $\mu = 0.332$. A silver addition of 3 % tended to lower the friction coefficient and the lowering of the friction coefficient became even more significant for the composite Ag-containing films grown at a temperature of 500 °C. The impact of silver incorporation into the basic CrN compound can be thus considered as slightly positive, when tested against bronze at room temperature.

Figure 7 shows an overview of the friction coefficients μ recorded while testing against alumina at a room and elevated temperatures. The normal load applied was

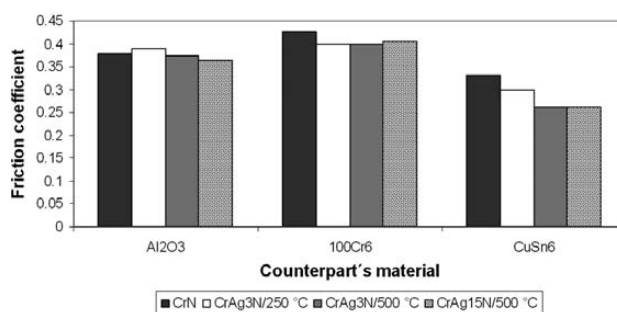


Figure 6: Average friction coefficient of investigated films against various counterpart materials, testing at room temperature, normal load applied of 1 N

Slika 6: Povprečni koeficient trenja za preiskovane nanose pri različnih materialih v paru, preizkušeno pri sobni temperaturi, normalna obremenitev 1 N

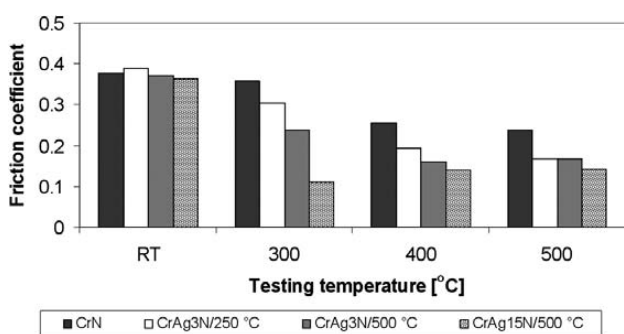


Figure 7: Average friction coefficient of investigated films against alumina at room (RT) and elevated temperatures, normal load applied of 1 N

Slika 7: Povprečni koeficient trenja za preiskovane nanose pri aluminijevem oksidu pri sobni temperaturi (RT) in povišanih temperaturah, normalna obremenitev 1 N

1 N. As stated above, almost no differences in μ were found when tested at room temperature. Testing at 300 °C, however, yields to a different behaviour of the coatings. The friction coefficients for the pure CrN, CrAg3N grown at 250 °C, CrAg3N grown at 500 °C and CrAg15N formed at 500 °C were 0.357, 0.304, 0.238 and 0.110, respectively. Higher testing temperatures lowered the difference in the μ for different coatings, for instance, the friction coefficients recorded by the testing at 400 °C were 0.256, 0.194, 0.160 and 0.139 for the pure CrN, CrAg3N formed at 250 °C, CrAg3N formed at 500 °C and CrAg15N formed at 500 °C, respectively. The measurement at 500 °C gave rather similar results.

Table 3 shows the wear rates calculated from the widths of the wear scars produced by the sliding of an alumina counterpart on the samples' surfaces. At room temperature the beneficial effect of the silver addition is evident only in the case of the CrAg3N film grown at 500 °C. Compared to pure CrN, the wear rate is lowered by two times. For the film containing 3 % Ag grown at 250 °C, a slight worsening of the wear rate was recorded and, for the film containing 15 % Ag the wear rate was higher by an order of magnitude.

The testing at elevated temperature led to a dramatic increase of the wear rate for the pure CrN film. The film with a 3 % Ag addition grown at 250 °C behaved in a very similar way from the qualitative point of view. The wear rate was minimal after the testing at an ambient temperature, which was followed by a steep increase at 300 °C and a decrease at 400 °C and 500 °C, respectively. However, it is clearly evident that the wear rates

after the testing at these temperatures are considerably lower. This makes a distinct difference compared to the wear behaviour of the pure CrN film. The film with the same silver content, but grown at 500 °C, had lower wear rates than that grown at 250 °C at room temperature and 300 °C, respectively. However, the testing at higher temperatures brought a higher wear rate. The film that contains 15 % Ag had the lowest wear rate when tested at 300 °C. However, the wear rate of the film increased as the testing temperature increased, and the increase of the wear rate was found to be greater than those of other investigated films.

The results of wear-rate measurements at room temperature are very consistent with the obtained values of the friction coefficients – the wear rate decreased with a decrease of the μ .

In order to explain the temperature behaviour of both coatings, it should be noted that there was no lubricant added to the experimental setup. The fact that the wear rate was lower or higher can thus be attributed only to the self-lubricating effect of the silver. This effect is, however, prevalent only above the testing temperature of 400 °C, when the Ag-atoms are capable of being transported to the surface.

Below this temperature, but above the ambient temperature, only the effect of the softening of the coatings can be expected. It was reflected by a much higher wear rate at 300 °C than that at ambient temperature. Finally, it should also be noted that the softening of alumina could take place during the testing.⁵¹ The behaviour of the film that contains 15 % Ag can be characterized as a special case. As we determined, the incorporation of 15 % Ag makes the film soft. This gives a natural explanation for the high wear rate measured at ambient temperature. At a temperature of 300 °C, the friction coefficient of the coating became extremely low and thereby the wear rate was lowered, also. Above this temperature, however, a softening of the coating can be expected, as reported for instance by Kostenbauer et al.⁴⁰ which gives a natural explanation for the high wear rate measured at 400 °C and 500 °C, respectively.

Figure 8 demonstrates the wear scars obtained by testing the CrAg3N and CrAg15N films developed at 500 °C, at ambient temperature. The testing gave very narrow tracks in the cases of CrN and CrAgN, respectively, see the representative micrograph in **Figure 8a**. The track developed on the CrAg15N film looks rather wider (**Figure 8b**), as a result of the lower hardness of

Table 3: Wear rate (mm³/(N m)) at ambient and elevated temperatures, alumina used as a counterpart

Tabela 3: Hitrost obrabe (mm³/(N m)) pri sobni in povišanih temperaturah; aluminijev oksid uporabljen kot par

Testing temperature coating (°C)	CrN	CrAg3N/ 250 °C	CrAg3N/ 500 °C	CrAg15N/ 500 °C
Room temperature	6.947×10^{-13}	7.399×10^{-13}	3.65×10^{-13}	1.031×10^{-12}
300	2.926×10^{-11}	2.894×10^{-11}	8.405×10^{-12}	7.053×10^{-12}
400	1.162×10^{-11}	4.329×10^{-12}	9.927×10^{-12}	1.925×10^{-11}
500	1.927×10^{-11}	6.208×10^{-12}	1.522×10^{-11}	4.802×10^{-11}

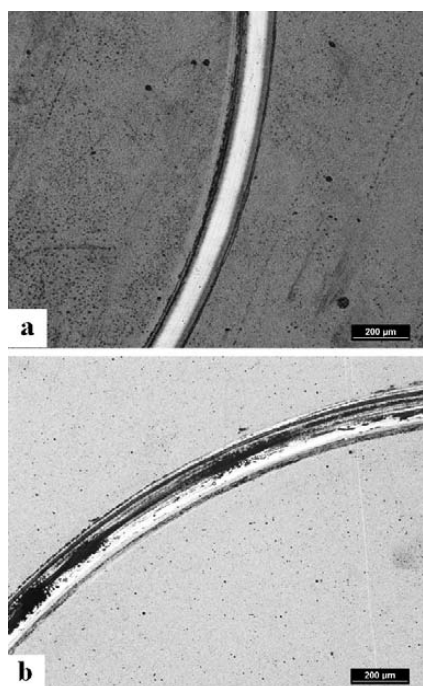


Figure 8: Light micrographs showing the wear tracks of: a) CrAg3N film grown at 500 °C, b) CrAg15N film grown at 500 °C, after sliding at room temperature, alumina used as a counterpart

Slika 8: Svetlobni posnetek prikazuje sledi obrabe: a) CrAg3N-nanos, nanosen pri 500 °C, b) CrAg15N-nanos, nanosen pri 500 °C, po drsenju pri sobni temperaturi, za par je bil uporabljen aluminijev oksid

the film. These results correspond well with the measured wear rates. The wear rates of the films formed with pure CrN and CrAg3N, respectively, were very low, while that of the CrAg15N film was considerably higher (Table 3).

Figure 9 shows representative optical images of the wear scars developed while testing the CrAg3N and CrAg15N films, respectively, against the alumina counterpart at various temperatures. Compared to the wear tracks obtained at ambient temperature, there is significant broadening visible. This can be due to the fact that the elevated temperature tends towards softening of the films. It should be noted that the softening of alumina could also be expected. However, the softening of the films probably became more remarkable.

The testing at 300 °C (Figures 9a and 9d), gave wear tracks of similar width, e.g., 0.267 mm and 0.251 mm for the CrAg3N and CrAg15N films, respectively. This can be considered rather surprising because the CrAg15N film is much softer than the CrAg3N and, further softening can be expected at higher temperature. However, the friction coefficient was measured to be much lower for the CrAg15N; this can be referred to the higher silver content in the CrN and its better capability to facilitate lubrication at higher temperatures, in good agreement with previous investigations.^{32,33,37}

The testing at 400 °C (Figures 9b and 9e) induced significant broadening of the wear tracks. This is high-

lighted for the CrAg15N film much more than that for CrAg3N, compare Figures 9b and 9e. Here, the effect of softening of CrAg15N became prevalent and the self-lubrication by Ag particles was insufficient to compensate for the softening of the film. It is worth noting that the opinions on the optimal silver content from the point of view of the self-lubricating effect facilitation are divergent. Hu et al.,³³ for instance, have reported that the minimal Ag amount in the coating was the mole fraction $x = 24\%$ to ensure lubrication at higher temperatures. Mulligan et al.⁵² have established that the optimal amount of silver incorporated into CrN is $x = 22\%$. This is quite enough for the formation of a lubricious film inside the wear tracks and for the achievement of an excellent tribological performance. In the current experiment, much lower silver additions were used. It is thus logical that this is the softening of the CrN through the Ag, which plays a dominant role in the tribological behaviour of the films.

The testing at 500 °C highlighted the differences between the tribological behaviour of the films containing 3 % and 15 % Ag, respectively (Figures 9c and 9f). The width of the wear track on the CrAg3N film

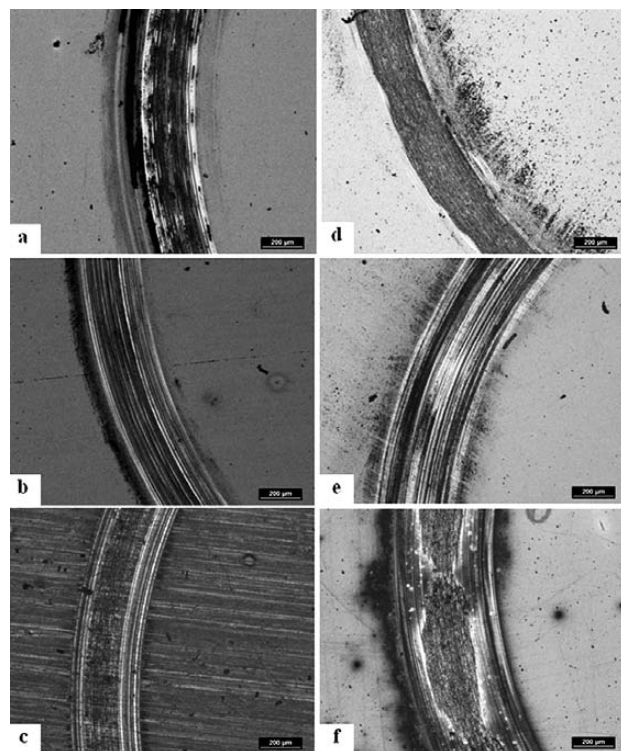


Figure 9: Plan-view optical images showing the wear tracks of the CrAg3N film grown at 500 °C: a) testing temperature of 300 °C, b) testing temperature of 400 °C, c) testing temperature of 500 °C and CrAg15N film grown at 500 °C, d) testing temperature of 300 °C, e) testing temperature of 400 °C, f) testing temperature of 500 °C

Slika 9: Svetlobni posnetki sledi obrabe na CrAg3N-nanosu, nanosenem pri 500 °C: a) temperatura preizkusa 300 °C, b) temperatura preizkusa 400 °C, c) temperatura preizkusa 500 °C in CrAg15N-nanos, nanosen pri 500 °C, d) temperatura preizkusa 300 °C, e) temperatura preizkusa 400 °C, f) temperatura preizkusa 500 °C

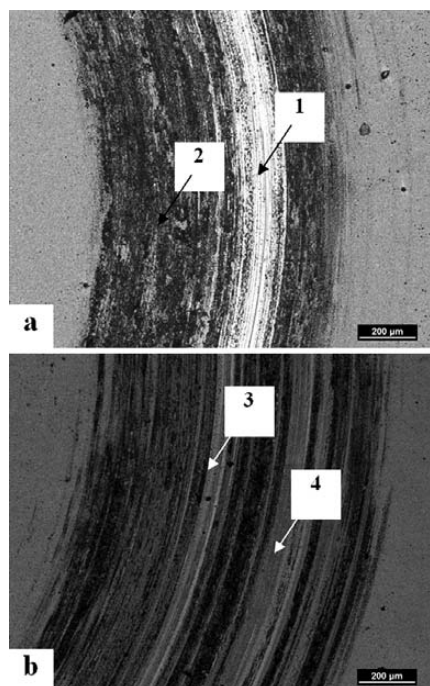


Figure 10: Plan view optical images showing the wear tracks of the CrAg₃N film grown at 500 °C, developed during contact with CuSn₆: a) testing at ambient temperature, b) testing temperature of 400 °C

Slika 10: Svetlobni posnetek sledov obrabe na CrAg₃N-nanosu, nastal med kontaktom s CuSn₆: a) preizkus pri sobni temperaturi, b) temperatura preizkusa 400 °C

increased to 0.324 mm. Here, no indications of total failure of the film were observed. The width of the films that contain 15 % Ag was 0.477 mm. There are indications of total film failure clearly visible – the free substrate surface is shown inside the wear scars.

Figure 10 shows representative plan-view micrographs of the wear tracks obtained by testing of CrAg₃N-film, grown at 500 °C, against the CuSn₆ ball. The testing at ambient temperature gave wear tracks with a width of 0.89 mm (**Figure 10a**). There are two typical areas inside the wear track. The first one can be clas-

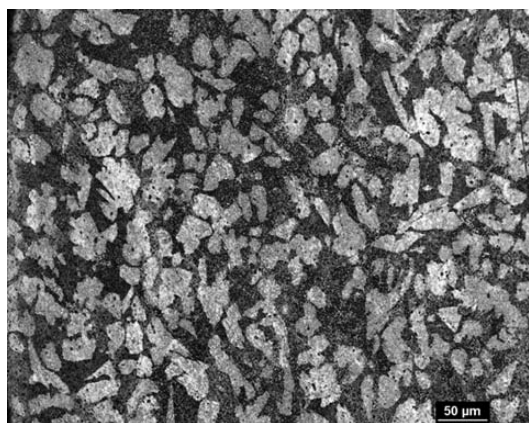


Figure 11: Light micrograph showing the microstructure of a CuSn₆ ball

Slika 11: Svetlobni posnetek mikrostrukture kroglice CuSn₆

sified as almost unaffected by the sliding (1). The second part of the wear track exhibits clearly visible symptoms of scraping (2). However, no evidence of the counterpart's adhesion was recorded.

The testing at a temperature of 400 °C produced wear tracks with a width of 1.02 mm (**Figure 10b**). Here, two typical areas inside the track can also be found. The first one is, similar to the case of the testing at a room temperature, almost unaffected by the sliding (3). The dominant part of the wear track, however, shows indications of considerable counterpart material transfer (4). The counterpart's material exhibits evidence of surface oxidation, because of the elevated temperature used for the testing.

To explain the behaviour of the sliding couple CrAg₃N deposited at 500 °C vs. CuSn₆ bronze, various aspects should be considered. First of all it should be noted that the behaviour of the sliding couple is determined by the fact that the CuSn₆ is soft in nature (149 HV 10) and it has a low shear strength, so that it can be easily smeared on the surface. This tendency is highlighted when a higher testing temperature is used. Moreover, the bronze does not contain any hard phases. **Figure 11** shows the microstructure of the CuSn₆ ball. The bright particles are the α -phase formations with an average microhardness of 156 HV (0.1) and the dark places are formed by the eutectoid $\alpha + \epsilon$, having an average microhardness of 196 HV (0.1). This is why no abrasive character of the interaction sample/counterpart has been detected. Moreover, the softness of the CuSn₆ has made it impossible to determine the wear rate using the method.⁴⁴ The measurement of wear profiles using profilometers was not possible, also. Therefore it can only be concluded that the CrAg₃N film exhibits good anti-sticking properties at low temperature, but that these properties are worsened at elevated temperatures.

4 CONCLUSIONS

Investigations of magnetron-sputtered CrN films with various Ag additions have brought the following findings:

The pure chromium nitride film grew in a typical columnar manner with clearly visible individual crystals. Its surface structure is a mixture of semi-equiaxed grains and cauliflower-like formations.

The addition of 3 % Ag tends mainly towards a refinement in the scale of the microstructural features, while the incorporation of 15 % Ag induced considerable changes in the growth manner, whereas no individual crystals of the CrN are more visible and nano-sized silver agglomerates are formed.

The pure CrN film as well as those with a 3 % Ag addition grew at a deposition rate of 720 nm/h, while the growth rate of the film with 15 % Ag was accelerated to 1050 nm/h. It is clear that the deposition temperature did not affect both the deposition rate and the final coating

thickness, but a higher Ag content led to a greater thickness of the film.

The nanohardness and the Young modulus of the pure CrN film were 16.79 GPa and 244 GPa, respectively. A small addition of silver has almost no impact on both the nanohardness and the Young's modulus. The incorporation of 15 % Ag into the film induced a reduction of both the nanohardness and the Young's modulus. There is probably a threshold of Ag content below which the impact of the silver on the mechanical properties of chromium nitride can be considered as negligible.

The addition of 3 % Ag improved the adhesion of the CrN film, whereas the improvement was considerably higher in the case of the film grown at 500 °C. The adhesion of the film with 15 % Ag was very poor.

It has been established that there is almost no effect of silver addition on the friction coefficient when tested at room temperature against alumina, but the testing against the same counterpart at higher temperature gave a positive effect of the silver addition on the μ .

The testing against 100Cr6 steel gave a higher friction coefficient than that against the alumina, while the testing against the CuSn6 bronze led to lower μ .

The addition of 3 % Ag to the CrN increased the wear performance at elevated temperatures, while the addition of 15 % Ag made the film too soft and sensitive to wear, which resulted in a partial removal of the film from the substrate inside the wear tracks.

Based on the obtained results, it seems that the optimal silver addition into the CrN film lies between 3 % and 15 %. Hence, silver concentrations of 7 % and 11 %, respectively, are going to be investigated (determination of the most important coating characteristics, i.e., microstructure, hardness, Young's modulus, wear resistance, friction coefficient) in the near future.

Acknowledgements

This paper is the result of the project implementation: CE for the development and application of diagnostic methods in the processing of metallic and non-metallic materials, ITMS: 26220120048.

5 REFERENCES

- R. Aubert, A. Gillet, J. Gaucher, P. Errat, *Thin Solid Films*, 108 (1983), 165
- R. Gahlin, M. Bromark, P. Hedenquist, S. Hogmark, G. Hakanson, *Surf. Coat. Techn.*, 76–77 (1995), 174
- A. Tricoteaux, P. Y. Jouan, J. D. Guerin, J. Martinez, A. Djouadi, *Surf. Coat. Techn.*, 174–175 (2003), 440
- G. Paller, B. Matthes, W. Herr, E. Broszeit, *Mater. Sci. Eng. A*, 140 (1991), 647
- L. Cunha, M. Andritshky, *Surf. Coat. Techn.*, 111 (1999), 158
- P. H. Mayrhofer, H. Willmann, C. Mitterer, *Surf. Coat. Techn.*, 146–147 (2001), 222
- A. Lousa, J. Romero, E. Martinez, J. Esteve, F. Montala, L. Carreras, *Surf. Coat. Techn.*, 146–147 (2001), 268
- A. Kondo, T. Oogami, K. Sato, Y. Tanaka, *Surf. Coat. Techn.*, 177–178 (2004), 238
- C. Nouveau, E. Jorand, C. Deces-Petit, C. Labidi, M. A. Djouadi, *Wear*, 258 (2005), 157
- C. Nouveau, M. A. Djouadi, C. Deces-Petit, P. Beer, M. Lambertin, *Surf. Coat. Techn.*, 142–144 (2001), 94
- O. Salas, K. Kearns, S. Carrera, J. J. Moore, *Surf. Coat. Techn.*, 172 (2003), 117
- W. K. Grant, C. Loomis, J. J. Moore, D. L. Olson, B. Mishra, A. J. Perry, *Surf. Coat. Techn.*, 86–87 (1996), 788
- M. Odén, J. Almer, G. Hakansson, M. Olsson, *Thin Solid Films*, 377–378 (2000), 407
- D. Mercs, N. Bonasso, S. Naamane, J. M. Bordes, C. Coddet, *Surf. Coat. Techn.*, 200 (2005), 403
- E. Martinez, J. Romero, A. Lousa, J. Esteve, *Surf. Coat. Techn.*, 163–164 (2003), 571
- S. M. Aouadi, D. M. Schultze, S. L. Rohde, K. C. Wong, K. A. R. Mitchell, *Surf. Coat. Techn.*, 140 (2001), 269
- L. Cunha, M. Andritshky, K. Pischow, Z. Wang, *Thin Solid Films*, 355–356 (1999), 465
- P. H. Mayrhofer, G. Tischler, C. Mitterer, *Surf. Coat. Techn.*, 142–144 (2001), 78
- M. A. Djouadi, C. Nouveau, P. Beer, M. Lambertin, *Surf. Coat. Techn.*, 133–134 (2000), 478
- R. Wei, E. Langa, C. H. Rincon, J. H. Arps, *Surf. Coat. Techn.*, 201 (2006), 4453
- J. Lin, Z. L. Wu, X. H. Zhang, B. Mishra, J. J. Moore, W. D. Sproul, *Thin Solid Films*, 517 (2009), 1887
- J. Lin, W. D. Sproul, J. J. Moore, S. Lee, S. Myers, *Surf. Coat. Techn.*, 205 (2011), 3226
- B. Warcholinski, A. Gilewicz, *Journal of Achievements in Materials and Manufacturing Engineering*, 37 (2009) 2, 498
- M. Béger, P. Jurči, P. Grgač, S. Mečiar, M. Kusý, J. Horník, *Kovove Materialy/Metallic Materiále*, 51 (2013) 1, 1
- A. P. Ehiassarian, W. D. Munz, L. Hultman, U. Helmersson, I. Petrov, *Surf. Coat. Techn.*, 163–164 (2003), 267
- J. W. Lee, S. K. Tien, Y. C. Kuo, C. M. Chen, *Surf. Coat. Techn.*, 200 (2006), 3330
- F. R. Lamastra, F. Leonardi, P. Montanari, F. Casadei, T. Valente, G. Gusmano, *Surf. Coat. Techn.*, 200 (2006), 6172
- E. Broszeit, C. Friedrich, G. Berg, *Surf. Coat. Techn.*, 115 (1999), 9
- F. Attar, T. Johannesson, *Thin Solid Films*, 258 (1995), 205
- R. R. Aharonov, B. F. Coll, R. P. Fontana, *Surf. Coat. Techn.*, 61 (1993), 223
- C. P. Mulligan, T. A. Blanchet, D. Gall, *Surf. Coat. Techn.*, 203 (2008), 584
- C. Muratore, A. A. Voevodin, J. J. Hu, J. S. Zabinski, *Wear*, 261 (2006), 797
- J. J. Hu, C. Muratore, A. A. Vojvodin, *Compos. Sci. Technol.*, 67 (2007), 336
- S. M. Aouadi, D. P. Singh, D. S. Stone, K. Polychronopoulou, F. Nahif, C. Rebholz, C. Muratore, A. A. Vojvodin, *Acta Mater.*, 58 (2010), 5316
- C. P. Mulligan, T. A. Blanchet, D. Gall, *Surf. Coat. Techn.*, 204 (2010), 1388
- C. P. Mulligan, D. Gall, *Surf. Coat. Techn.*, 200 (2005), 1495
- C. P. Mulligan, T. A. Blanchet, D. Gall, *Surf. Coat. Techn.*, 205 (2010), 1350
- S. M. Aouadi, A. Bohnhoff, M. Sodergren, D. Mihut, S. L. Rohde, J. Xu, S. R. Mishra, *Surf. Coat. Techn.*, 201 (2006), 418
- P. Basnyat, B. Luster, Z. Kertzman, S. Stadler, P. Kohli, S. Aouadi, J. Xu, S. R. Mishra, O. L. Eryilmaz, A. Erdemir, *Surf. Coat. Techn.*, 202 (2007), 1011
- H. Kostenbauer, G. A. Fontalvo, J. Keckes, C. Mitterer, *Thin Solid Films*, 516 (2008), 1920

- ⁴¹ P. Jurči, B. Šuštaršič, V. Leskovšek, *Mater. Tehnol.*, 44 (2010) 2, 77–84
- ⁴² A. I. Tyshchenko, W. Theisen, A. Oppenkowski, S. Siebert, O. N. Razumov, A. P. Skoblik, V. A. Sirosh, Y. N. Petrov, V. G. Gavriljuk, *Mater. Sci. Eng., A*, 527 (2010), 7027
- ⁴³ A. Oppenkowski, S. Weber, W. Theisen, *J. Mater. Proc. Technol.*, 210 (2010), 1949
- ⁴⁴ ASTM G 99-95a Standard Test Method for Wear Testing with a Pin-on-Disk Apparatus, ASTM International, 2000
- ⁴⁵ P. Jurči, *Mater. Tehnol.*, 45 (2011) 5, 383–394
- ⁴⁶ S. H. Yao, Y. L. Su, W. H. Kao, K. W. Cheb, *Surf. Coat. Technol.*, 201 (2006), 2520
- ⁴⁷ P. Jurči, I. Dlouhý, *Appl. Surf. Sci.*, 257 (2011) 24, 10581
- ⁴⁸ P. Jurči, S. Krum, *Materiálové inžinierstvo/Materials Engineering*, 19 (2012) 2, 64
- ⁴⁹ N. Schell, J. H. Petersen, J. Bottiger, M. Mucklich, J. Chevallier, K. P. Andreasen, F. Eichhorn, *Thin Solid Films*, 426 (2003), 100
- ⁵⁰ Z. B. Zhao, Z. U. Rek, S. M. Yalisove, J. C. Bilello, *Surf. Coat. Technol.*, 185 (2004), 329
- ⁵¹ R. G. Munro, *J. Am. Ceram. Soc.*, 80 (1997), 1919
- ⁵² C. P. Mulligan, T. A. Blanchet, D. Gall, *Wear*, 269 (2010), 125